Pergamon

PII: S0191-8141(97)00100-4

Journal of Structural Geology, Vol. 20, No. 4, pp. 363 to 370, 1998

0191-8141/98 $19.00 + 0.00

Strains at the intersections of synchronous conjugate normal faults

J. WATTERSON, A. NICOL*, J. J. WALSH

Fault Analysis Group, Department of Earth Sciences, University of Liverpool, Liverpool L69 3BX, U.K.

and

D. MEIER

82 Mindener Str., D-32469 Petershagen, Germany

(*Received* 25 *April* 1997; *accepted in revised form* 10 *October* 1997)

Abstract—Processes accommodating the mutual offsetting of intersecting conjugate faults are investigated by outcrop examination of three pairs of conjugate normal faults with maximum throws from 5 mm to 10 cm. In two cases resolved fault throws decrease sharply towards the intersection zones which, on the scale of observation, are zones of ductile thinning of inter-fault layers that accommodate the throw reductions. Strain within the intersection zone of conjugate faults in fluvio-glacial sands is accommodated by inter-grain slip, and layer thinning is complemented by layer-parallel extension at constant volume. In a second example, strain within the intersection zone of conjugate faults in inter-layered chalk and marl is accommodated by volume reduction, without layer extension. In a third example, also in fluvio-glacial sands, strain in the intersection zone is accommodated by small faults (throws $\geq$1 mm); when throws on all resolvable faults are aggregated, there is no decrease in throw towards the conjugate intersection. The presence or absence of a decrease in resolved throw towards conjugate intersections and of a complementary ductile zone accommodating the change in throw, is a function not only of the resolution limit of the observations but also of the scale of the deformation process within the conjugate zone. © 1998 Elsevier Science Ltd. All rights reserved

INTRODUCTION

Many fault systems comprise conjugate sets of faults, which can accommodate a pure shear bulk deformation (Freund, 1974; Horsfield, 1980; Ramsay and Huber, 1987). While intersections between conjugate faults do not represent a geometrical problem, they pose an apparent kinematic problem if both faults were active at the same time. In brief, what happens in the region where the two faults intersect and offset one another? On the basis of the limited resolution afforded by seismic data, Nicol *et al.* (1995) showed that the displacements on a pair of conjugate normal faults apparently decrease towards an intersection zone, within which there is ductile thinning and extension. It was further suggested that this ductile strain was accommodated by arrays of sub-seismic minor faults which formed as a consequence of the repeated offsetting of each of the conjugate faults by the other. The decrease in resolved displacement on the seismically mapped conjugates towards their intersection is, therefore, only an apparent decrease as the 'missing' displacement is simply accommodated on many sub-seismic offsets in the intersection zone. Nicol *et al.* (1995) also noted that a component of the ductile strain in the intersection region could be accommodated by other processes, such as the pressure solution described by Odonne and Massonnat (1992) in an outcrop example of intersecting conjugate faults in carbonates.

The purpose of this paper is to investigate the geometries and strains in the intersection regions of outcrop-scale conjugate faults, thus avoiding the resolution limitations of seismic data. Cross-section data are available for three conjugate intersection structures, in one case in the form of serial sections. Strains in the intersection regions of these three structures are shown to be accommodated predominantly by inter-grain slip, by multiple cross-cutting faults, and by volume loss, respectively. The three examples are consistent with normal dip-slip displacements, in the range *ca* 1 mm–115 mm, but this may not always be the case. A conjugate structure is illustrated which cannot be interpreted in terms of dip-slip displacement alone.

INTER-GRAIN SLIP

Figures 1 and 2 show conjugate normal faults within a block (*ca* 18 × 12 × 20 cm) extracted from layered (1–5 mm) Pleistocene fluvio-glacial sands at Nienburg, Germany. The conjugate faults post-date an early thrust (Fig. 2) and have normal dip-slip separations with throws ranging up to 11 mm (Fig. 3a & b). Six serial sections (Fig. 2), approximately perpendicular to the strike of the main faults (NNE–SSW), provide a degree of three-dimensional control on the geometries and displacements of the faults.

* Present address: Institute of Geological and Nuclear Sciences Ltd, PO Box 30 368, Lower Hutt, New Zealand. e-mail fault@fag.esc.liv.ac.uk

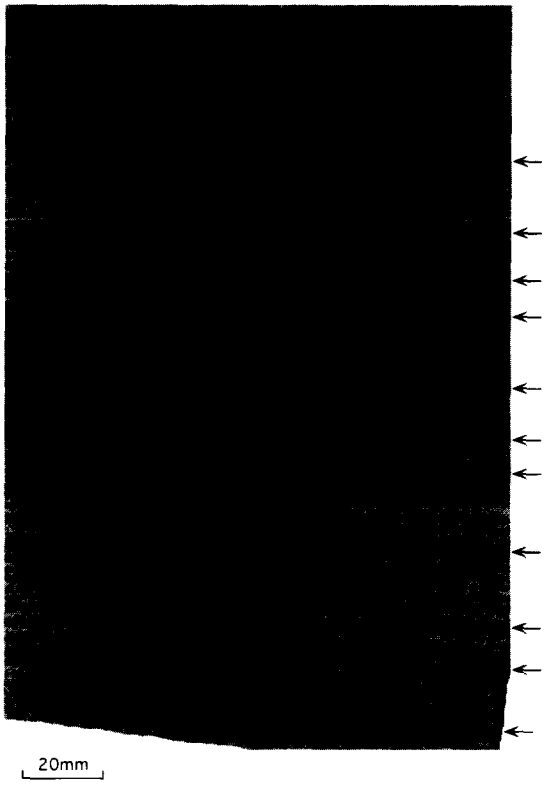

Fig. 1. Intersecting conjugate faults in Pleistocene fluvio-glacial sands from Nienburg, Germany (see Section 4, Fig. 2, for interpretation). Arrows show horizons on line drawing of Fig. 2.

The sections show progressive changes in the geometries of the main faults and in the symmetry of the conjugate structure (Fig. 2) from an inverted 'y' structure with a right-dipping dominant fault (Sections 1–3), through an 'X' shaped conjugate structure (Sections 2–5), to an asymmetric 'X' shaped structure with a left-dipping dominant fault which is more continuous and has slightly larger displacements than the right-dipping fault (Section 6). The existence of a more or less symmetrical 'X' shaped conjugate along only a part of the intersection line is as would be expected from Meier (1993), Nicol *et al.* (1995) and Walsh *et al.* (1996).

Displacement contour diagrams for faults A and B (Fig. 3a & b) were constructed from the cross-section data. Within the volume examined, the maximum throw on fault A (*ca* 11 mm) is approximately twice that of fault B (*ca* 5 mm). Displacements on Fault B decrease from Section 6 towards Section 1 and those on Fault A increase in that direction. Maximum displacements on both faults lie below the intersection line, consistent with the faults having intersected at a point where both were propagating upwards and sideways (see fig. 6 of Woods, 1988; Nicol *et al.*, 1996); Fault A towards Section 6 and Fault B towards Section 1 within the imaged volume. The shallow plunge of the intersection line (Fig. 3) is consistent with the faults having similar strike directions. Displacement contours on Faults A and B and on the aggregate displacement diagram (Fig. 3a–c) become more nearly parallel to the intersection line as they approach it, reflecting the pronounced zones of low displacement on both faults adjacent to the intersection line. The way in which this zone of apparently low displacement is accommodated is shown by thickness changes of individual layers across the faults, expressed as strain indices (Fig. 4, see text to figure for definition of strain index). Complete strain index profiles can be drawn only for Sections 3, 4 and 5. Figure 4 shows that within 15 mm above and below the intersection point, the layers between the two faults (mutual hangingwall above the intersection and mutual footwall below it) have been thinned by 10–45%. As area-balancing of individual layers in each cross section provides no indication of volume loss, a corresponding extension of these inter-fault layers is assumed. The ductile strain increases from Section 3 through Section 4 to Section 5, where the conjugate structure is most symmetrical. As no fault offset greater than 0.5 mm (the estimated limit of resolution) can be seen in these strained inter-fault layers, it is inferred that inter-granular slip accommodated the extension of up to 40% in the inter-fault region, within 10–15 mm of the intersection. Inter-grain slip was the deformation mechanism observed in the experiments of Horsfield (1980). Ductile strain of the intersection zone accommodates the decreases in fault displacements towards the intersection line. This type of ductile strain in the intersection zone is illustrated by the change in shape of a nominally rectangular area defined at the time of initiation of the conjugate structure (Fig. 5a & b).

VOLUME LOSS

An intersecting pair of conjugate faults (Fig. 6a) outcrops in a cliff section of interbedded layers of Cretaceous chalk (*ca* 1 mm–1.5 m thick) and marl (*ca* 1 mm–8 cm thick) at Danes Dyke, Flamborough Head, Yorkshire, U.K. The location and fault systematics are described more fully in Peacock and Sanderson (1992, 1994) and in Childs *et al.* (1996). Strikes of both faults are in the range 120°–150°, and both have normal dip-slip displacements with throws up to *ca* 10 cm. Each fault trace consists of a series of sub-parallel segments, offset from one another and each terminating at either a marl horizon or at a pronounced bedding-plane discontinuity (Fig. 6a).

In the section exposed, the conjugate structure is asymmetric with fault trace A dominant by virtue of its greater length and higher maximum throw. On both fault traces throw decreases towards both the upper and lower margins of the area illustrated in Fig. 6(a) although only one tip-point is seen where fault trace B terminates at the base of a thin marl layer. It is assumed that the other decreases in throw towards the upper and lower margins of Fig. 6(a) also indicate the proximity of tip-points. However, throws on both faults also decrease sharply towards their intersection, as illustrated in the throw profiles (Fig. 6b). The aggregate throw profile (fault

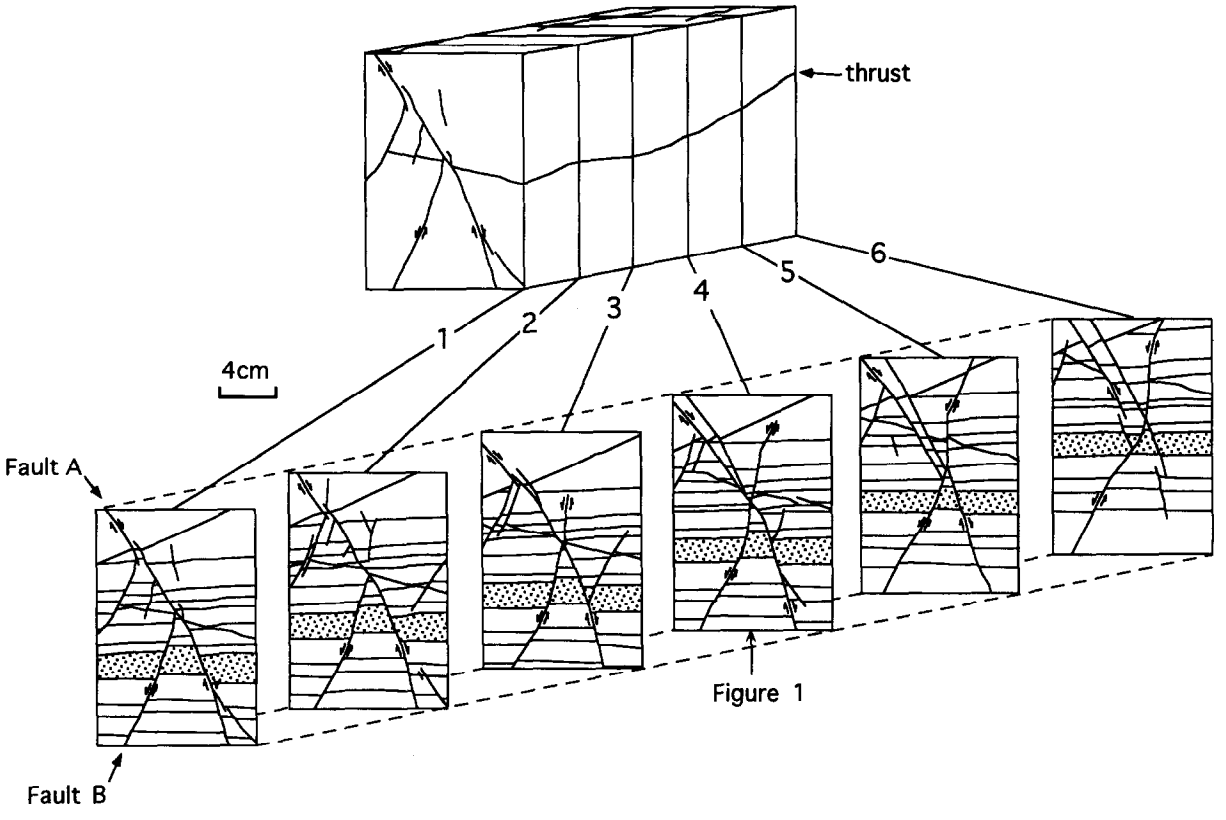

Fig. 2. Block diagram and serial sections (1–6) drawn from photographs (e.g. Fig. 1) showing three-dimensional geometries of conjugate faults and of horizons used in displacement analysis (Fig. 3). Sections are vertical, normal to the strike of the main conjugate faults and at approximately 4 cm intervals. Vertical and horizontal scales are equal.

traces A + B + C) shows an apparent throw deficit at the intersection of *ca* 75% relative to the minimum expected throw, as estimated from the profiles from > 40 cm above and from > 60 cm below the intersection point. The throw deficit is complemented by up to *ca* 30% relative thinning of inter-fault layers in the intersection region. There are few identifiable faults (throw resolution *ca* 1 mm) in the intersection region and certainly not sufficient to compensate for the sharp decreases in throw on the faults shown in Fig. 6(a). The high gradients of throw (0.061–1.0, mean *ca* 0.14) which characterise the decreases in throw towards the intersection zone are accommodated mainly by thinning of the inter-fault layers achieved by volume loss and complemented by subordinate extension. Volume loss in the intersection region was estimated by measuring the area loss on the basis of a bed by bed restoration, maintaining fixed fault positions. The estimated area loss of up to 40% within the intersection zone (Fig. 7) is subject to potential error due to possible irregularity of bedding traces prior to faulting, and does not take account of the possible prior dilatation which is expected to accompany inter-grain slip deformation. Volume loss is likely to have been dominantly by pressure solution along bed-parallel seams. Volume and porosity reduction by collapse of delicate coccolith plate structures, a common means of volume reduction elsewhere (e.g. Koestler and Ehrmann, 1987), is unlikely because prior to deformation Yorkshire chalk underwent impregnation by secondary calcite and reduction of porosity to 8–17% from likely original values of 40–50% (Mimran, 1978). The relative increases in areas of inter-fault layers (Fig. 7) towards the top and bottom of the cross section illustrated in Fig. 6(a) accommodate the throw decreases associated with the observed and inferred tip-points which are also accommodated by volume loss. Similar area, or volume, changes are described by Odonne and Massonnat (1992) who, from outcrop observations of a conjugate structure in limestone, show that the greatest losses of area by pressure solution are associated with intersections and tip-points of conjugate fault traces. This type of strain in the intersection zone is illustrated by the change in shape and area of a nominally rectangular area defined at the time of initiation of the conjugate structure (Fig. 5a & c).

MULTIPLE CROSS-CUTTING FAULTS

A cross section through an array of intersecting conjugate faults in Pleistocene fluvio–glacial sands at Freden, Germany, is shown in Fig. 8a. In this section the fault traces dip steeply (65°–85°) and form a broadly 'X' shaped structure, with between two and five traces

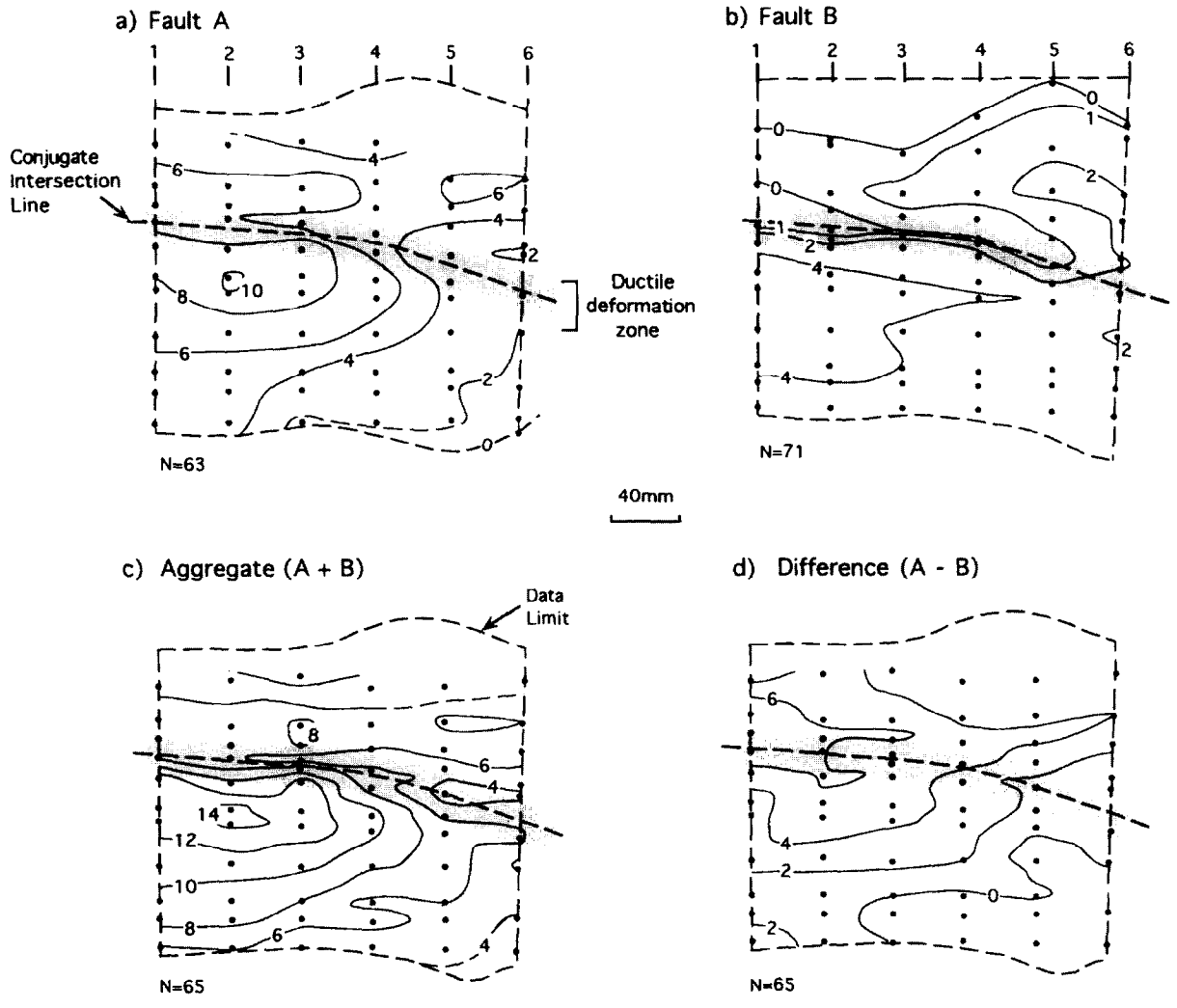

Fig. 3. (a) and (b) Throw (mm) contoured fault-surface maps for faults A and B (see Fig. 2). Displacements on both strands of fault A are aggregated. (c) Contoured aggregate of throws (mm) on Faults A and B. (d) Contour differences between throws (mm) on Faults A and B. Section locations are indicated at the top of each diagram. Vertical and horizontal scales are equal.

comprising each composite fault. The faults have normal dip-slip separations with throws on individual traces ranging up to *ca* 3.2 cm. Aggregate throws are approximately the same on each composite fault, but are higher above the intersection (4–4.5 cm) than below it (3–3.3 cm); the lower aggregate throws below the intersection are largely compensated by bed rotations. The conjugate arrays are mutually cross cutting with individual traces offset by one or more younger traces of opposing dip (Fig. 8a). The array of cross-cutting faults accommodates a vertical thinning and associated horizontal extension of the interval which straddles the intersection zone (stippled in Fig. 8). There is relatively little internal deformation or rotation of fault bounded areas. Cross-cutting relationships allow the relative timing of slip to be established for each fault strand which passes through the intersection zone. This relative chronology provided a basis for the restoration of fault displacements which was carried out using the assumption of rigid fault block translation, modified where necessary by minor bed rotations. The simplifying assumption of rigid blocks does not allow account to be taken of displacement changes along fault traces. The youngest fault strand was restored first and the oldest last. Layer thickness variations are small (< 1–2 mm) and provide good control on the restoration process. Displacements on fault traces which terminate in free tip-points, as opposed to branch-points, were either relayed onto the closest fault (fault 1, fault 2 and fault 3, Fig. 8a) or the fault trace was extrapolated to the boundary of the section (fault 4, Fig. 8a). The relative ages of faults which do not pass through the intersection zone are uncertain, so their associated displacements and bed rotations were restored last.

A minimum of 10 alternations between left (first) and right (last) dipping fault restorations is necessary to unfault the conjugate structure. Figure 8(b & c) show an intermediate stage and the final stage of restoration, respectively. Restoration of some individual fault strands requires a minimum of five slip events. Rigid block

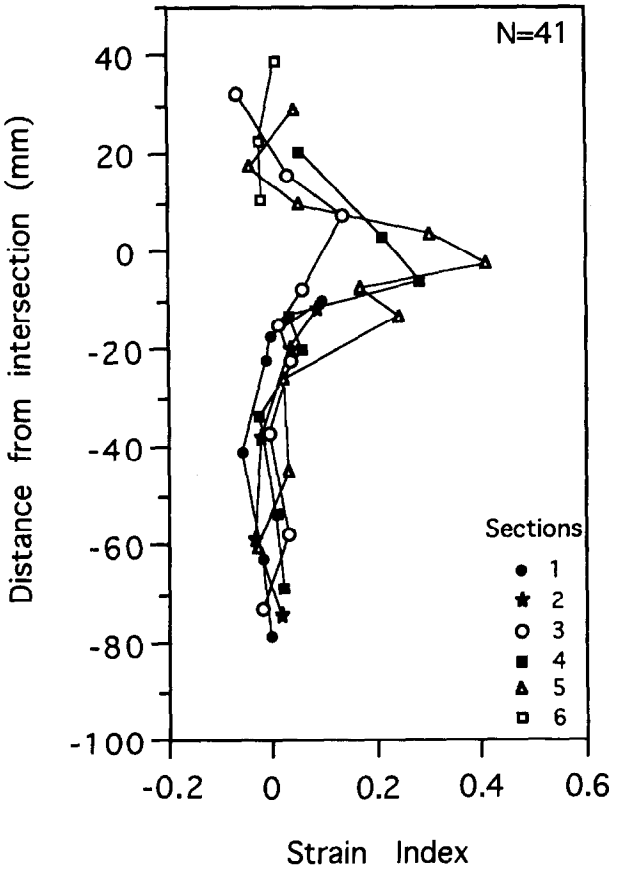

Fig. 4. Plot of vertical distance from fault intersection vs strain index for layers in each cross section (1–6) in Fig. 2. The strain index (SI) is defined by $SI = (T1-T2)/T1$ where $T1$ = average thickness of a layer outside the conjugate structure and $T2$ = average thickness of same layer between the faults (i.e. in either the mutual hangingwall or the mutual footwall). SI values for layers thickened by the thrust in the mutual hangingwall are omitted. Distances are vertical distances from the intersection to the mid point of each layer.

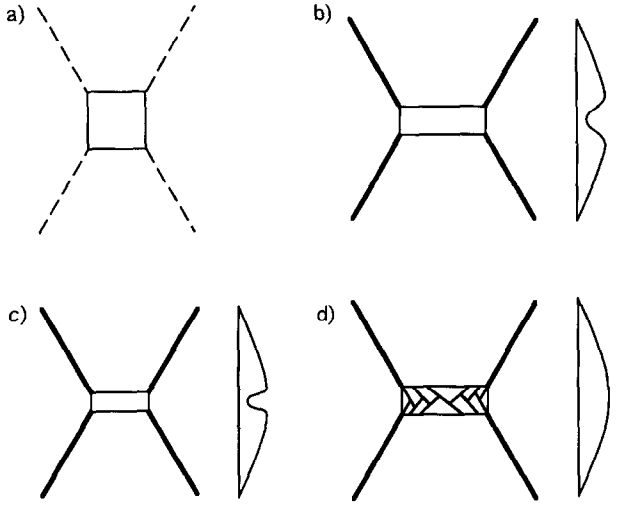

Fig. 5. Schematic diagram illustrating the different strains of an initially rectangular region at the intersection of two conjugate faults, due to different deformation mechanisms. The diagram is not to scale and the fault-trace lengths are unrealistically short. Profiles of aggregate resolved throws are shown. (a) Rectangular region prior to fault development. (b) Strain in intersection region accommodated by sub-resolution deformation mechanisms with no volumetric strain (i.e. no volume reduction). (c) Strain in intersection region accommodated by pressure solution with negative volumetric strain (i.e. volume reduction). (d) Strain in intersection region accommodated by numerous small resolved faults, shown schematically and without continuation beyond the initial rectangular region, and with no volumetric strain. For a less diagrammatic version see Nicol *et al.* (1995)(fig. 13).

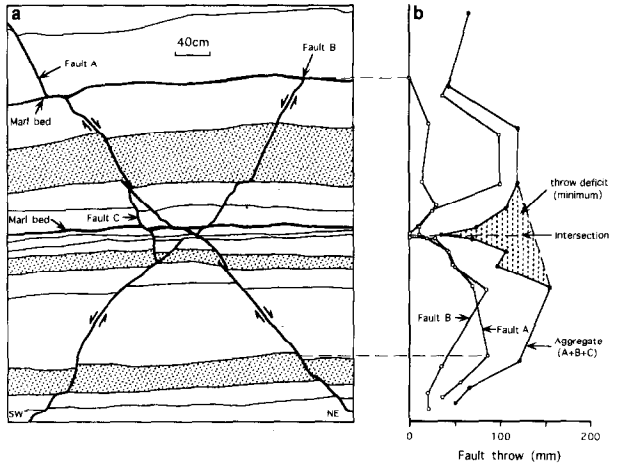

Fig. 6. (a) Intersecting conjugate faults in a vertical outcrop of interbedded (bed thicknesses *ca* 1 mm–1.5 m) Cretaceous chalk and marl at Danes Dyke, Yorkshire, U.K. Stippled and non-ornamented beds are chalk. (b) Throw profiles for Faults A and B and the aggregate throw profile for Faults A, B and C. Data point elevations on the aggregate profile are midway between the elevations on each of the aggregated faults.

restoration of the section creates only minor space problems in the form of voids (diagonal-line shading) and overlaps (horizontal-line shading) which are due mainly to changes in fault dip across the intersection (Fig. 8a–c). Voids and overlaps together account for $< 1\%$ of the total area and approximately balance. Rigid block restoration is relatively successful because there is relatively little ductile deformation within the cross section, consistent with the low gradients of fault displacement. Small (< 3 mm) residual offsets of the lowermost horizon shown in Fig. 8(c) probably reflect a minor component of ductile deformation close to the intersection.

Comparison of Fig. 8(a & c) indicates that faulting accommodated *ca* 24% horizontal extension across the section. The success of the restoration confirms the validity of a relative chronology in which fault strands become younger towards the middle of the conjugate structure, consistent with results of physical modelling (Horsfield, 1980; Woods, 1988).

Growth of the conjugate structure was associated with a widening of the array of faults at the intersection. On the left side of the structure at least, successively younger slip surfaces merge with the main fault progressively further from the intersection. The restoration is consistent with this structure having formed principally by translation of rigid fault blocks along multiple cross-cutting faults (Freund, 1974; Horsfield, 1980; Woods, 1988; Zhao and Johnson, 1991; Meier, 1993; Walsh *et al.*,

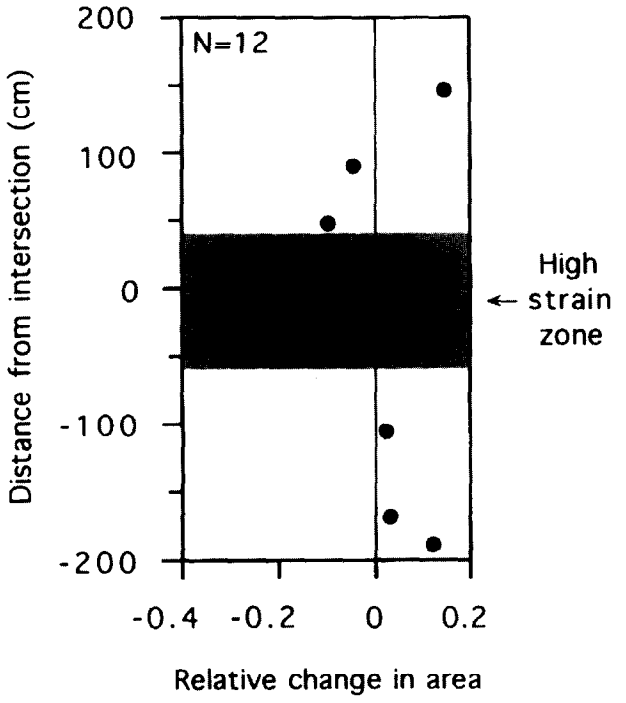

Fig. 7. Vertical distance from the intersection of the faults vs differences in bed areas per unit length across conjugate faults shown in Fig. 6. The difference in area is calculated by taking as fixed the positions of beds outside the conjugate faults, and restoring the fault displacements in the plane of the section. Values are expressed as positive or negative changes in area according to whether beds are thinner (negative) or thicker (positive) in the inter-fault region. Vertical distance is measured from the intersection to the mid point of a bed.

1996), with only minor bed rotation and ductile strain. If the data resolution was not good enough for the small faults in the intersection zone to be identified, the strain would be ductile and similar to that represented in Fig. 5(b).

It is not clear why the two examples of conjugate faults in fluvio–glacial sands should show such different deformation styles. The apparent similarity of the host materials could be deceptive if one was frozen when the faults formed. Alternatively, the difference could reflect the different amounts of strain in the two cases, other than that accommodated by displacements on the principal faults. Sandbox models show both an increasing number of faults (both main array faults and intersection zone minor faults) and a greater complexity of faulting at higher values of extension (Horsfield, 1980; Woods, 1988).

DISCUSSION AND CONCLUSIONS

Although all displacement changes on faults are accommodated by strain of the adjacent rock volume (Barnett *et al.*, 1987), the vertical displacement gradients and associated strains at conjugate-fault intersections are often considerably higher than those characteristic of single faults (Walsh and Watterson, 1989; Nicol *et al.*, 1996).

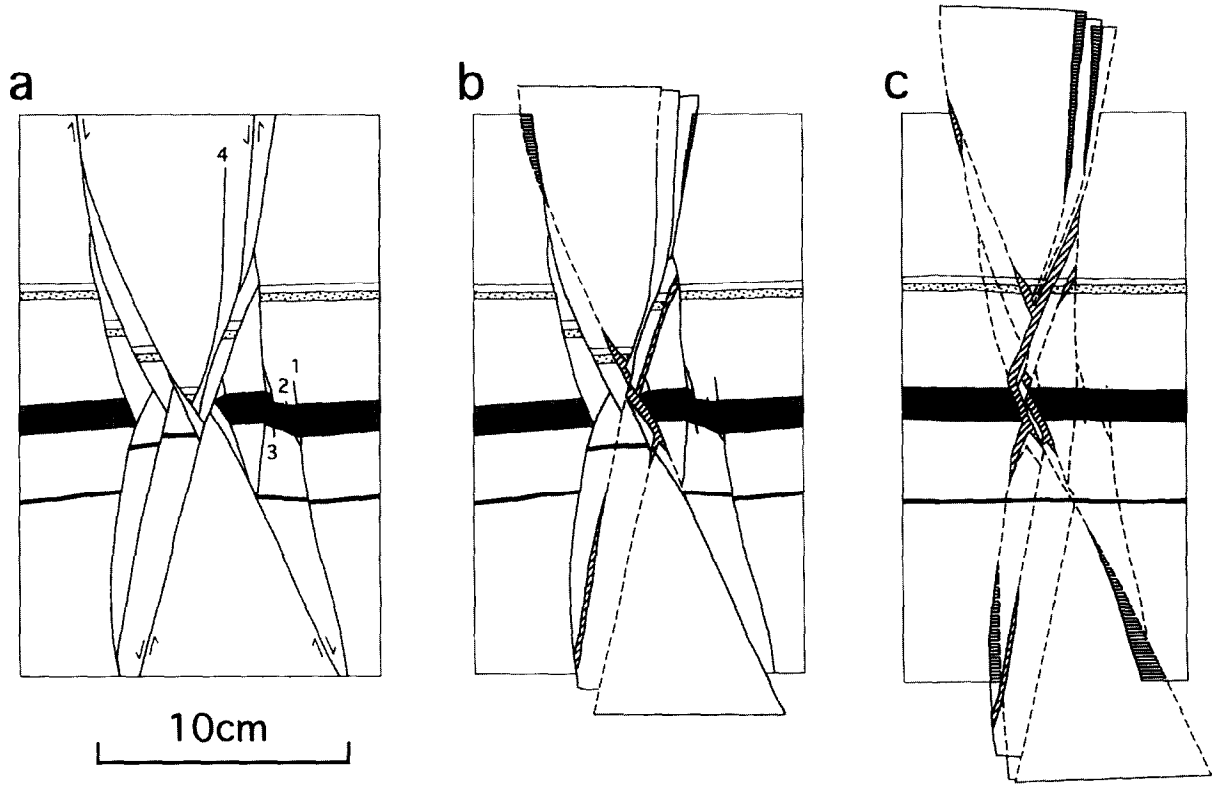

Fig. 8. (a) Conjugate normal faults in Pleistocene fluvio-glacial sands, Freden, Germany. (b) and (c) Sequential area balanced restorations of (a) by backstripping fault displacements using rigid-block translations. (b) After restoration of *ca* 12% extension and five fault slip events. (c) Restored to pre-faulting state, i.e. after *ca* 24% extension and ≥10 slip events. See text for restoration procedure.

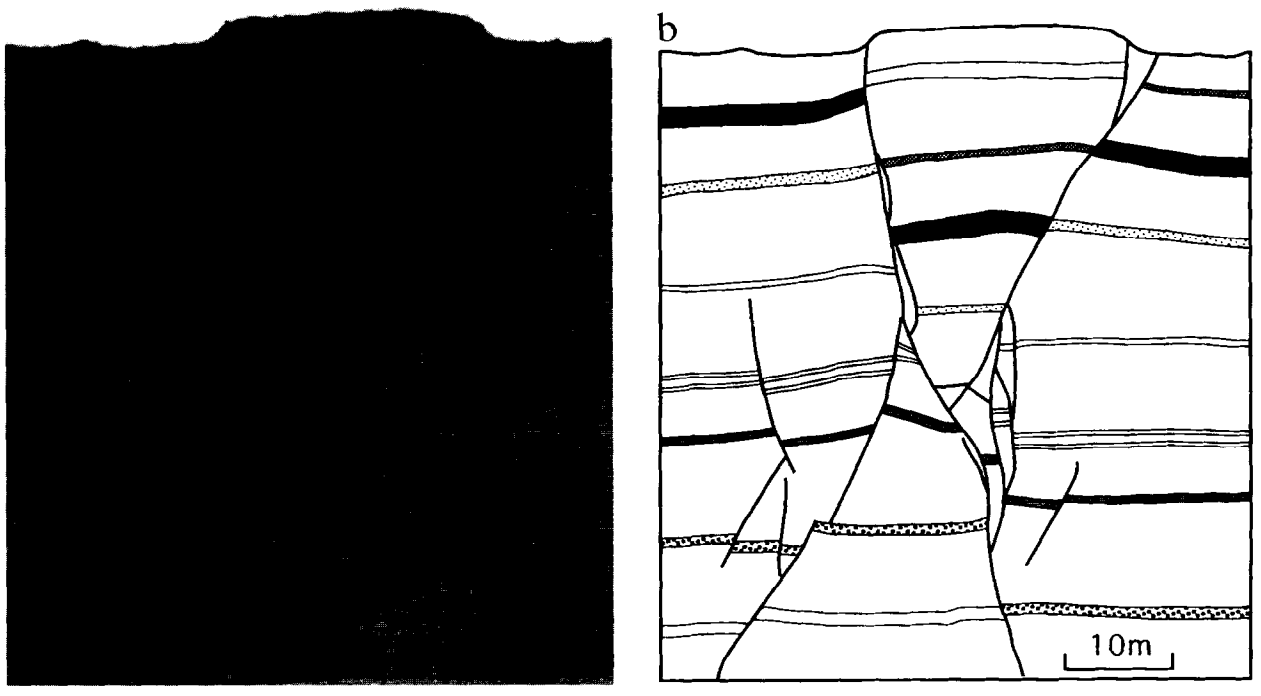

Fig. 9. (a) Intersecting conjugate faults exposed in a 60 m high vertical cliff of Liassic limestone, Nash Point, South Wales. The sequence is well defined and horizon correlations across the faults are unambiguous. (b) Horizon and fault trace interpretation of (a).

The conjugate structures shown in Figs 3 and 6 show rapid decreases in throw of 30–100% towards the intersection zones. These decreases in throw are accommodated by strains which, on the scale of observation, are ductile, i.e. inter-grain slip and volume loss. On the structure illustrated in Fig. 8, on the other hand, where nearly all the strain is accommodated by structures above the limit of resolution, i.e. small faults, there is no decrease in throw towards the conjugate intersection. Had this structure been examined at a scale with a higher resolution limit, say 5 cm throw, there would be an apparent decrease in resolved throw towards the conjugate intersection and a corresponding component of ductile strain would need to be invoked. Displacement decreases and ductile strains associated with seismically imaged conjugate faults have been attributed to resolution effects (Nicol *et al.*, 1995). In such cases it is not possible to determine objectively which sub-resolution deformation process or processes is responsible, although sub-seismic faulting is likely to be the most common. Whether or not apparent decreases in resolved throw toward a conjugate intersection are observed (together with an associated ductile strain of the intersection zone) is, therefore, a function not only of the scale of observation, or resolution limit, but also of the scale of the deformation mechanism in the intersection zone.

Although the three examples we have illustrated can each be interpreted as the product of exclusively normal faulting, it is emphasised that not all conjugate structures are the products of normal-fault movement alone. For example, displacement geometries on the conjugate structure shown in Fig. 9 cannot be reconciled with dip-slip movement alone and a strike-slip component is confirmed by near-horizontal ($<20°$) fibres and slickenside striations on both of the main faults illustrated.

Acknowledgements—We are grateful to Conrad Childs and Paul Gillespie for discussion and to Marie Eeles for preparation of diagrams. James Mendelsshon of Atlantic College, South Wales, drew our attention to the conjugate faults at Nash Point (Fig. 9), while Paul Gillespie provided the interpretation of this example (Fig. 9b). Significant improvements resulted from a review by Manuel Willemse. This research was part funded by the DTI/NERC Hydrocarbon Reservoirs LINK Programme (project 827/7053), and by the EU Hydrocarbon Reservoir Research Programme (contract JOUF3-CT95-0006).

REFERENCES

Barnett, J. A. M., Mortimer, J., Rippon, J. H., Walsh, J. J. and Watterson, J. (1987) Displacement geometry in the volume containing a single normal fault. *Bulletin of the American Association of Petroleum Geologists* **71**, 925–937.

Childs, C., Nicol, A., Walsh, J. J. and Watterson, J. (1996) Growth of vertically segmented normal faults. *Journal of Structural Geology* **18**, 1389–1397.

Freund, R. (1974) Kinematics of transform and transcurrent faults. *Tectonophysics* **21**, 93–134.

Horsfield, W. T. (1980) Contemporaneous movement along crossing conjugate normal faults. *Journal of Structural Geology* **2**, 305–310.

Koestler, A. G. and Ehrmann, W. U. (1987) Fractured chalk overburden of a salt diapir, Laegerdorf, NW Germany—exposed exam-

ple of possible hydrocarbon reservoir. In *Dynamical Geology of Salt and Related Structures*, ed. I. Lerche and J. J. O'Brien, pp. 457–477. Academic Press, London.

Meier, D. (1993) *Abschiebungen: Geometrie und Entwicklung von storungen im Extensionsregime*. Ferdinand Enke Verlag, Stuttgart.

Mimran, Y. (1978) The induration of Upper Cretaceous Yorkshire and Irish chalks. *Sedimentary Geology* **20**, 141–164.

Nicol, A., Walsh, J. J., Watterson, J. and Bretan, P. G. (1995) Three-dimensional geometry and growth of conjugate normal faults. *Journal of Structural Geology* **17**, 847–862.

Nicol, A., Watterson, J., Walsh, J. J. and Childs, C. (1996) The shapes, major axis orientations and displacement patterns of fault surfaces. *Journal of Structural Geology* **18**, 235–248.

Odonne, F. and Massonnat, G. (1992) Volume loss and deformation around conjugate fractures: comparison between a natural example and analogue experiments. *Journal of Structural Geology* **14**, 963–972.

Peacock, D. C. P. and Sanderson, D. J. (1992) Effects of layering and anisotropy on fault geometry. *Journal of the Geological Society of London* **149**, 793–802.

Peacock, D. C. P. and Sanderson, D. J. (1994) Strain and scaling of faults in the chalk at Flamborough Head, U.K *Journal of Structural Geology* **16**, 97–107.

Ramsay, J. G. and Huber, M. I. (1987) *The Techniques of Modern Structural Geology. Volume 2: Folds and Fractures*. Academic Press, London.

Walsh, J. J. and Watterson, J. (1989) Displacement gradients on fault surfaces. *Journal of Structural Geology* **11**, 307–316.

Walsh, J. J., Watterson, J., Childs, C. and Nicol, A. (1996) Ductile strain effects in the analysis of seismic interpretations of normal fault systems. In *Modern Developments in Structural Interpretation, validation and Modelling*, ed. P. G. Buchanan and D. A. Nieuwland, pp. 27–40. Special Publication of the Geological Society of London 99.

Woods, E. P. (1988) Extensional structures of the Jabiru Terrace. In *The North West Shelf, Australia*, ed. P. G. and R. R. Purcell, pp. 311–330. Proceedings of the Exploration Society of Australia Symposium, Perth, 1988.

Zhao, G. and Johnson, A. M. (1991) Sequential and incremental formation of conjugate sets of faults. *Journal of Structural Geology* **13**, 887–895.